JOURNAL OF GEOPHYSICAL RESEARCH, VOL. 93, NO. A10, PAGES 11,455–11,472, OCTOBER 1, 1988

Subionospheric VLF Signatures of Nighttime D Region Perturbations in the Vicinity of Lightning Discharges

U. S. INAN, D. C. SHAFER, AND W. Y. YIP

Space Telecommunications and Radioscience Laboratory, Stanford University, Stanford, California

R. E. ORVILLE

Department of Atmospheric Science, State University of New York, Albany

A 12-hour sequence of perturbations of subionospheric VLF signals observed in association with lightning provided preliminary evidence that the ionospheric regions perturbed in these events may be confined to within ~ 150 km of the lightning discharges, and that intracloud flashes as well as cloud-to-ground lightning may be important in producing the perturbations. High-resolution analysis of event signatures indicated the presence of two different classes of events. For one set of events, observed during the most active central 6 hours of the observation period, a ~ 0.6-s delay between the causative lightning and VLF event onset and a ~ 1-s onset duration was observed, consistent with previously suggested models of the gyroresonant whistler-particle interaction that leads to particle precipitation and perturbation of the Earth-ionosphere waveguide. However, another set of events, observed during the first 2 hours of the observation period, exhibited a very different temporal signature, characterized by a much smaller (< 50 ms) delay and sometimes also very short (< 50 ms) rise times. Such events are possibly related to previously reported cases of similarly early/fast events and may involve a more direct coupling between the lightning discharge and the lower ionosphere.

1. INTRODUCTION

In recent years, much has been learned about subionospheric VLF signatures of a type of transient ionospheric perturbation that appears to be caused by a burst of energetic (> 40 keV) electrons [*Inan and Carpenter*, 1987, and references therein]. The ionospheric perturbation, indicated schematically in Figure 1*c*, gives rise to changes in the amplitude and/or phase of subionospherically propagating waves. These changes, frequently called "Trimpi" events, have been correlated with the detection of whistlers from lightning [*Helliwell et al.*, 1973], and a growing body of information suggests that such burst electron precipitation is regularly induced as the result of a gyroresonant scattering interaction between whistler waves and the magnetospheric particle distribution. Figures 1*a* and 1*b* provide a simple descriptive model of the postulated process by which whistler wave energy, propagating along a particular discrete, or ducted, magnetospheric path, gives rise to localized precipitation regions at the ionospheric projections of a high-altitude wave-particle interaction region [*Helliwell et al.*, 1973; *Lohrey and Kaiser*, 1979; *Carpenter and LaBelle*, 1982].

Study of the Trimpi phenomenon has advanced rapidly in recent years through the investigation of subionospheric VLF signal perturbations at southern hemisphere stations, particularly Palmer ($L \sim 2.4$) and Siple, Antarctica ($L \sim 4.3$) [*Leyser et al.*, 1984; *Inan et al.*, 1985*a*; *Inan and Carpenter*, 1986, 1987; *Carpenter and Inan*, 1987], through direct detection on satellites of precipitating electrons associated with the propagation of whistlers [*Voss et al.*, 1984], and through rocket-based observations [*Goldberg et al.*, 1986].

The richness of the southern hemisphere ground data appears to be based on a combination of strong whistler lightning source activity in the opposite hemisphere (lightning activity near Palmer and Siple is minimal) and the proximity of the South Atlantic magnetic anomaly, as a result of which particles perturbed in a gyroresonance interaction with south-going whistler waves are precipitated into the southern hemisphere ionosphere after first mirroring and/or backscattering in the north [*Chang and Inan*, 1983, 1985]. This type of precipitation has been referred to as "mirrored" precipitation, as opposed to "direct" precipitation. Direct precipitation, when observed in the southern hemisphere, would be due to north-going echoes of whistlers originating in northern hemisphere lightning or single hop whistlers (rare near Palmer) excited by lightning in the south [*Inan and Carpenter*, 1986]. At the longitudes of the eastern United States, and for lightning sources in the north, mirrored precipitation is believed to be significantly more effective (i.e., higher precipitated flux levels are expected) than direct precipitation [*Inan et al.*, 1988].

Observations in the northern hemisphere and hence in the vicinity of the causative lightning activity and wave injection allows the investigation of additional aspects of the Trimpi phenomenon, such as its distribution between hemispheres and the relations between the path of a perturbed signal and the location and intensity of a correlated lightning flash. Data from the northern hemisphere can be used to study the consistency of the observations with existing models of a gyroresonant interaction, the scattering role of nonducted as opposed to ducted whistler wave energy, the spatial size and distribution of precipitation regions, and the sensitivity of the subionospheric signals to off-great-circle ionospheric perturbations. It can also be used to study the differences in

Copyright 1988 by the American Geophysical Union.

Paper number 7A9351.
0148-0227/88/007A-9351$05.00

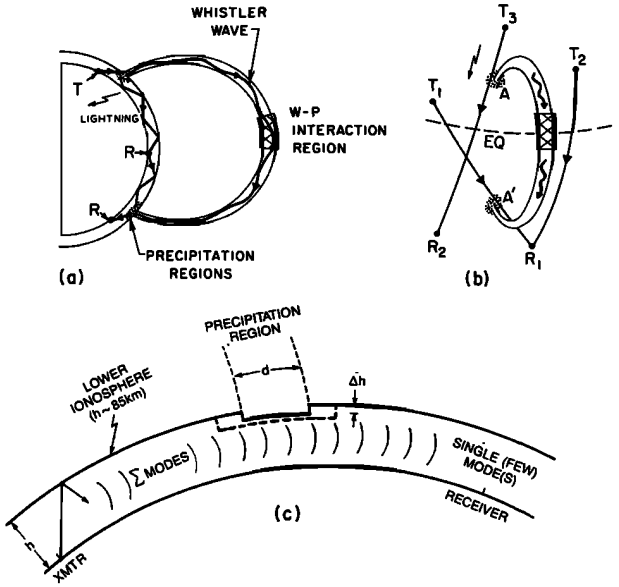

Fig. 1. Phenomenology of Trimpi events: (*a*) meridional plane projection of the field line of propagation showing a whistler wave launched by a lightning discharge propagating up the field line and interacting with energetic electrons in the vicinity of the equator; also shown is a subionospheric VLF/LF propagation path from a transmitter (T) to receiver(s) (R), (*b*) a three-dimensional sketch showing the spatial relationship of the whistler mode duct and subionospheric signal paths between transmitters (T_1, T_2, T_3) and receivers (R_1, R_2) that cross the precipitation regions (A, A'), and (*c*) a two-dimensional cross-sectional view of subionospheric propagation between a transmitter and receiver in the presence of a localized precipitation region, represented as a reduction Δh in the effective reflection height of the ionosphere over a region of length d.

the time signatures of the events as observed in the opposite hemispheres [e.g., *Chang and Inan*, 1985], and furthermore, to look for "early" effects, that is, effects that occur following the causative lightning within < 100 ms and hence within a small fraction of the magnetospheric transit time of the wave. These effects might be the result of a scattering interaction at low altitudes, near the particle mirror points, or may indicate some type of direct coupling between the lightning discharge and the lower D region. Previous evidence for such early effects include observations in the Antarctic of a case of Trimpi effects with essentially no delay from the associated atmospheric [*Armstrong*, 1983], and observations of large transient electric fields from lightning on a rocket near ionospheric altitudes of ~ 150 km [*Kelley et al.*, 1985].

In this paper we present some initial results from high-time-resolution monitoring of multiple signal paths in the northern hemisphere. Information on Trimpi events is for the first time combined with data on the location and intensity of correlated lightning. We present a case study of a 12-hour sequence of subionospheric VLF perturbation events observed in direct association with individual cloud-to-ground (CG) lightning flashes. The results provide evidence that the ionospheric region(s) perturbed in individual events may be centered within ± 150 km of the subionospheric propagation path, and that intracloud (IC) as well as cloud-to-ground (CG) flashes may be associated with VLF perturbation events. Of particular interest is the fact that while events observed during most of the 12-hour period exhibited temporal signatures (such as onset delay from causative spheric and duration of onset) consistent with theoretical models of a high-altitude gyroresonant whistler-particle interaction in the magnetosphere, events observed during the first $\sim 1\frac{1}{2}$ hours exhibited temporal signatures indicative of early effects as mentioned above, possibly due to some type of fast coupling between the thundercloud and the lower ionosphere.

2. Description of the Experiments

The VLF data described here were acquired at Lake Mistissini (LM), Quebec (50° N, 74° W, $L \simeq 4.9$), as part of the Stanford University program of subionospheric VLF/LF observations in the northern hemisphere. The geometry of the observations and sample subionospheric signal paths monitored are shown in Figure 2*a*. The LM observation program was started in November 1986, and continuous high-resolution recordings began in March 1987. Data are typically acquired during nighttime for ~ 14-hour periods (typically 2200-1200 UT or 1800-0800 MLT). Amplitudes of the VLF/LF signals are measured using narrowband receivers with a bandwidth of ~ 300 Hz. The detected envelopes of the receiver outputs are sampled at a basic rate of 100 Hz. Averaging on site is used to obtain the lower sampling rates (typically 20 or 50 Hz) at which the data are recorded on digital tape.

In addition, synoptic broadband (0-30 kHz) VLF recordings are made for 1 min out of every 5 or 15 min. These data are recorded on analog tape and are used for measure-

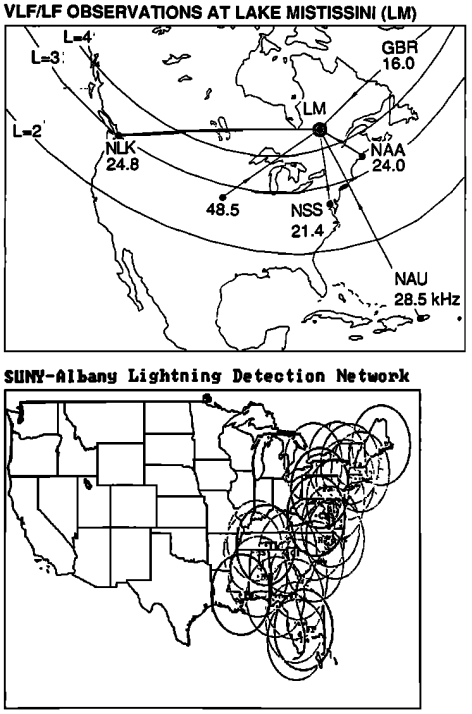

Fig. 2. (*a*) Observation geometry and sample signal paths measured at Lake Mistissini, Quebec, as part of the Stanford University program of subionospheric VLF/LF observations in the northern hemipshere. The loci of the footprint of the $L = 2, 3$, and 4 geomagnetic field lines at 100 km are also shown. (*b*) The coverage of the SUNY-Albany east-coast lightning-detection network during March 1987. Each circle represents a nominal direction finder range of 400 km.

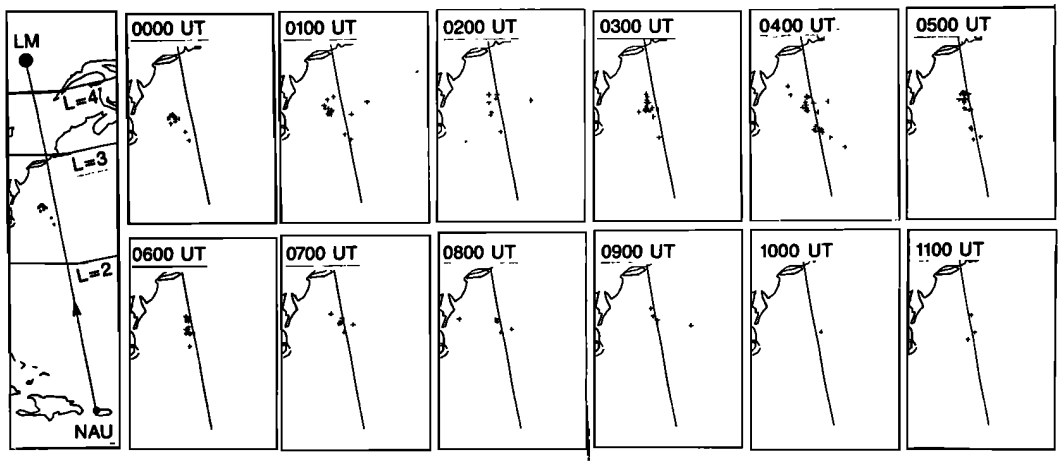

Fig. 3. Evolution of a localized thunderstorm as represented by cloud-to-ground (CG) lightning flash (pluses) occurrence during 0000-1200 UT on March 13, 1987. The great-circle propagation path between the NAU transmitter (28.5 kHz) in Aguadilla, Puerto Rico, and Lake Mistissini, Quebec, is shown for reference. The loci of the footprint of the $L = 2,3$, and 4 field lines at 100 km are also shown in the leftmost column.

ment of the frequency spectrum of spherics and whistlers (see Figures 11, 12 and 14).

The SUNY-Albany east-coast lightning-detection network has been in operation since 1982. The system is designed to detect and locate cloud-to-ground (CG) lightning flashes occurring within the region of coverage shown in Figure 2*b*. Intracloud (IC) flashes are not recorded, since the processing electronics are designed to respond only to those field shapes that are characteristic of return strokes in cloud-to-ground flashes [*Orville et al.*, 1987].

3. VLF Perturbation Events and Their Association With Lightning

In this section we summarize the salient features of the observed VLF activity and then compare with (1) CG flashes detected by the lightning-detection network, and (2) both CG and IC lightning activity as represented by radio atmospherics detected at LM with the VLF receivers.

Overview of VLF Event Activity

The March 13, 1987, case was selected for study because a large number of very well defined VLF events were observed over an extended period of time. This unusual characteristic may have been the result of a number of different factors having to do with the nature of the thunderstorm activity and with ionospheric or magnetospheric conditions. Apparently important was the fact that a single storm center with large, positive flashes (positive charge lowered to ground) persisted in the Atlantic Ocean ~ 400 km from the U.S. east coast for an extended period of time, essentially through all of the nighttime VLF recording period at Lake Mistissini. The development of this thunderstorm, as represented by the occurrence of cloud-to-ground (CG) flashes, is shown in Figure 3 in relation to the great-circle propagation path between the 28.5 kHz NAU transmitter in Aquadilla, Puerto Rico and Lake Mistissini, Quebec. The CG lightning activity during this period was evidently confined to within ± 150 km of the NAU-LM path; the distribution of electrical storm centers were extended along the VLF propagation path. Furthermore, the lightning activity seems to be centered near $L \simeq 2.5$, at an L shell where lightning-induced electron precipitation events are known to occur frequently [*Carpenter and Inan*, 1987; *Imhof et al.*, 1985].

A summary of the VLF activity observed during March 13, 1987, is presented in Figures 4 and 5. The data for the middle 6 hours (0300-0900 UT or 2300-0500 MLT) of the 12-hour period of observations are shown in Figure 4, while that for the preceding (0000-0300 UT) and the following (0900-1200 UT) 3 hours are given in Figure 5. For each hour, the amplitude of the 28.5-kHz NAU signal at LM is plotted in the top panels. The lower panels show the CG lightning data as discussed below. While the VLF signal amplitude was highly variable over different time scales throughout this period, the characteristic perturbations of interest were identified on the basis of their previously established temporal signature, involving a particularly rapid (< 1 s) onset followed by a relatively slow (10-100 s) recovery [*Inan and Carpenter*, 1986]. Amplitude changes with such signatures and with perturbation sizes of $> 1\%$ were counted as VLF events for the purpose of the statistical summary presented below in Figures 6-9.

As also discussed below, the nature of the VLF events changed during the observation period. During the first $\sim 1\frac{1}{2}$ hour of observations (Figure 5), events were characterized with positive steplike changes. High-resolution analyses of these events (section 4 below) revealed early/fast signatures, possibly indicating some type of direct coupling between the lightning discharges and the lower ionosphere. Events observed during the prime observation period of 0300-0900 UT were mostly negative amplitude changes and when analyzed at high-resolution (section 4) exhibited characteristic temporal signatures consistent with those expected for electron precipitation resulting from a gyroresonant whistler-particle interaction in the magnetosphere. The transition from the positive amplitude changes to the negative ones occurred during 0100-0200 UT. However, events observed during the transition period were generally small amplitude changes and, as a result, it was not posssible to make accurate measurements of temporal fea-

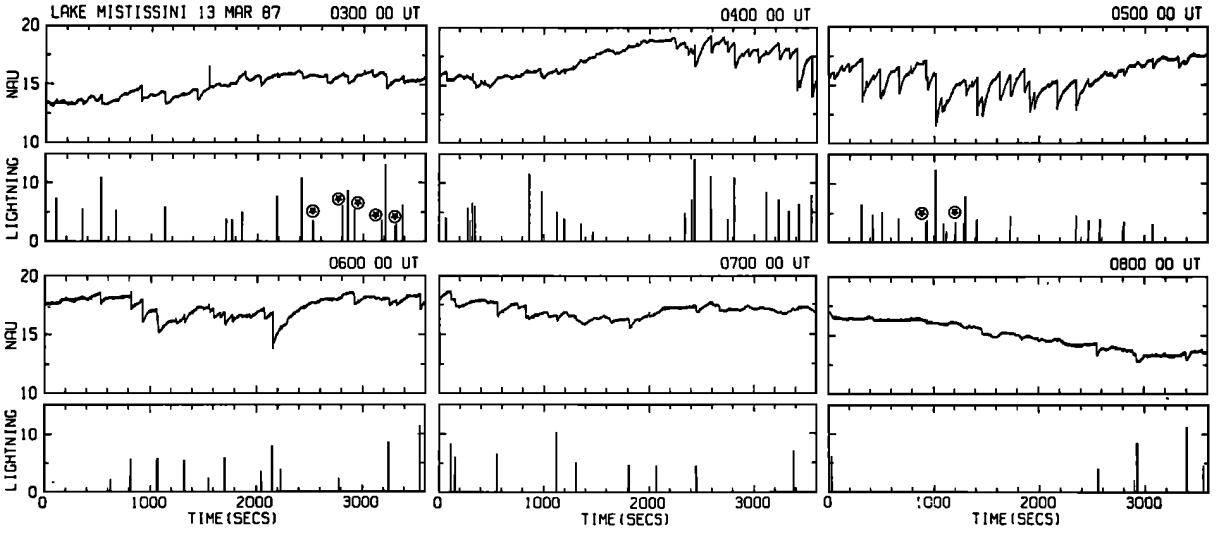

Fig. 4. Comparison of VLF activity recorded at LM with cloud-to-ground (CG) lightning activity detected by the SUNY-Albany network observed during 0300-0900 UT on March 13, 1987. For each hour, the top panel shows the intensity (A) of the 28.5-kHz NAU signal in linear arbitrary units, with $A = 0$ representing the absence of the signal, as measured within a bandwidth of $\sim$ 300 Hz and time-averaged over 1.28 s. The lower panels show the time of occurence (with 1-s resolution) and intensity where 10 corresponds to a peak current of 200 kA for CG flashes detected by the lightning network. Most of the CG flashes were positive (i.e., positive charge lowered to ground). The negative ones are identified with a circled cross. The time $t = 0$ corresponds to the UT given in the upper right corner.

tures from high resolution displays. Events were also observed during the last 3 hours (0900-1200 UT) as shown in Figure 5; however, these events were also generally small amplitude changes and again high resolution analyses were not useful. However, we note that such small events, identified on the basis of their rapid onset and slow recoveries as mentioned above, were included in the statistical summary presented below in Figures 6-9.

During the 1000-1100 UT period (Figure 5) the NAU signal amplitude goes through a maximum and a minimum followed by a subsequent slow decrease in the signal level during 1100-1200 UT. Such behavior is characteristic of day/night transition signatures on subionospheric VLF signals and results from the constructive/destructive interference between the sky wave signal components reflected from two different reflection heights as the day/night terminator moves across the propagation path [*Crombie et al.*, 1958]. Once the path is sunlit, the signal level decreases rapidly due to increased absorption as the D region ionization builds up with increasing solar illumination. No VLF events are observed during the 1100-1200 period when the NAU-LM path is sunlit. However, as shown below, the lightning activity has considerably decreased by this time, so that it is not possible to determine whether the lack of events during

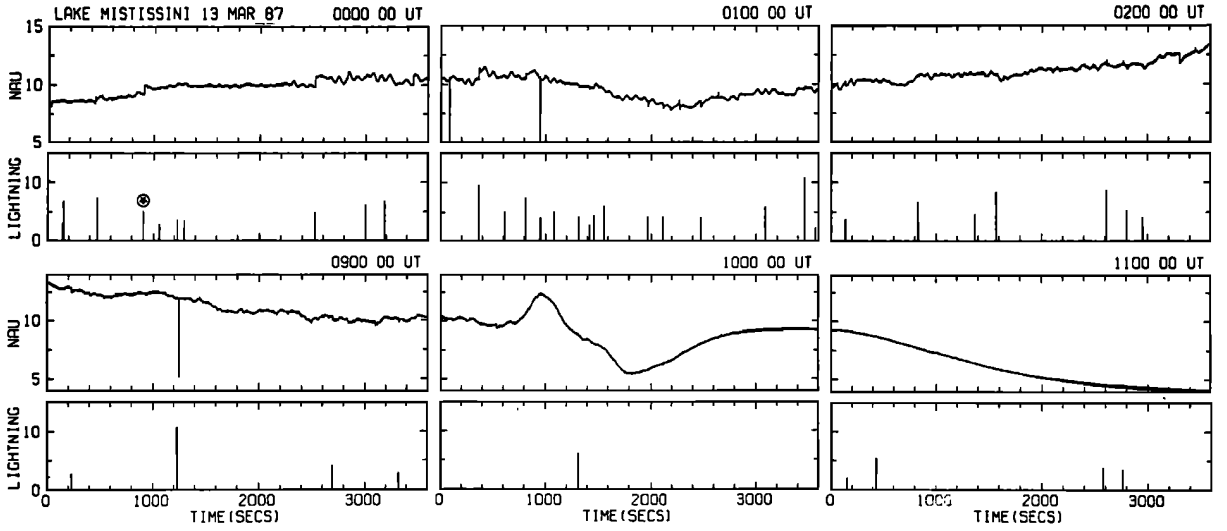

Fig. 5. Comparison of VLF activity with cloud-to-ground (CG) lightning activity observed during 0000-0300 and 0900-1200 UT on March 13, 1987, preceding and following the period of Figure 4. The format of the figure is identical to that of Figure 4.

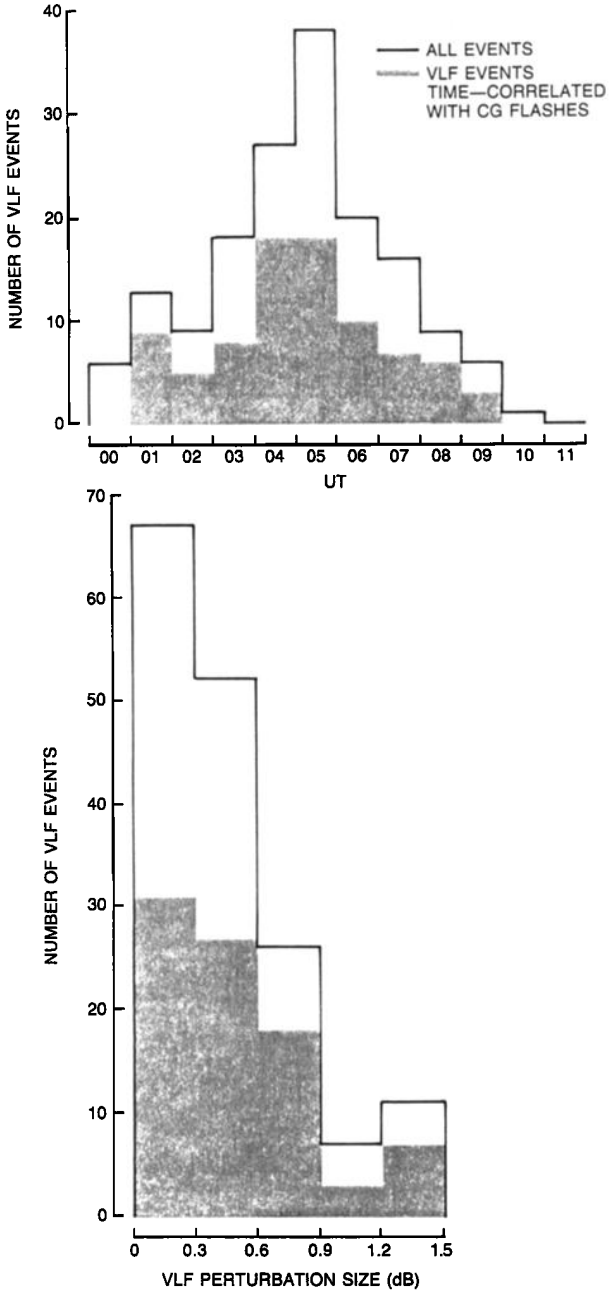

Fig. 6. Distribution of VLF events as a function of time (top panel) and in terms of perturbation size in decibels (bottom panel). The solid lines represent all of the VLF events identified on the basis of the characteristic signature (rapid (< 1 s) onset followed by slow (> 10 s) decay and perturbation size > 1%), whereas shading shows the number of VLF events which were time-correlated (< 1 s) with CG flashes.

this period is due to sunlit conditions along the propagation path.

In the following we jointly analyze the VLF events and the CG lightning both in terms of their time correlation and in terms of the distance between the location of the CG flash and the NAU-LM path.

Cloud-to-Ground (CG) Lightning

For each hour in Figures 4 and 5, the lightning data from the SUNY-Albany network is shown in the lower panels. The display is in the form of vertical spikes at the occurrence times of the CG flashes (with 1-s resolution); the spike intensity is proportional to the peak current in the first return stroke. The ordinate values in Figures 4 and 5 are derived by dividing by 100 the original uncalibrated wideband high gain direction finder units normalized to 100 km. From *Orville et al.* [1987], 1000 of the latter units correspond to approximately 200 kA. Thus the value 10 in the figures represents a peak current of 200 kA.

A general correspondence between VLF event activity and CG flash rate is evident from Figure 4. A particularly large and well-defined sequence of VLF perturbations started at ~ 0440 UT, at which time a sequence of relatively intense CG flashes also started. During 0800–0900 UT, when CG lightning activity was considerably reduced, the number of

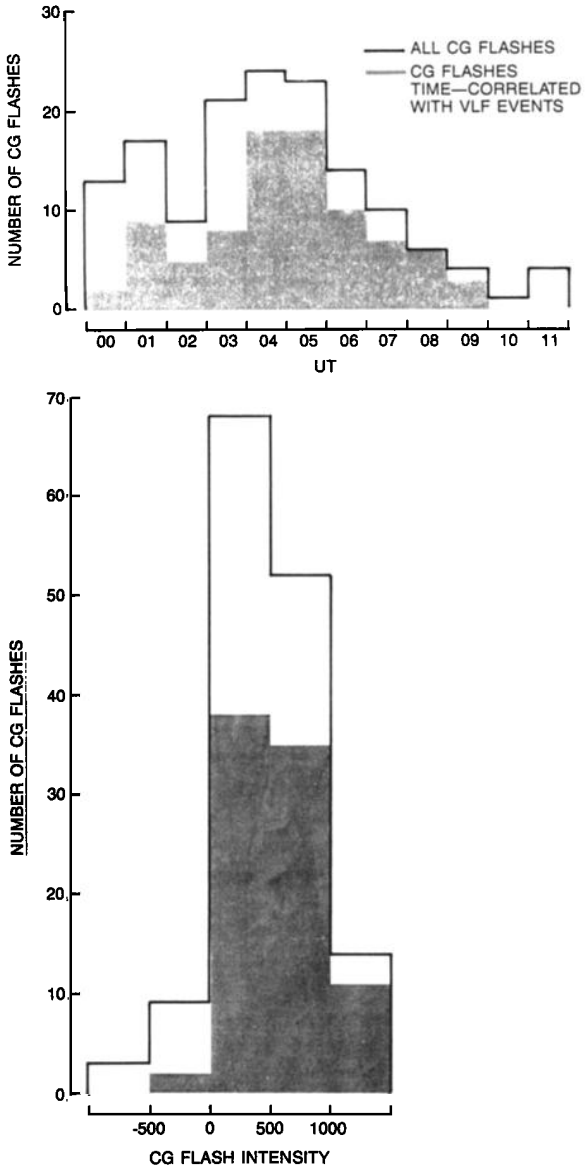

Fig. 7. Distribution of CG flashes as a function of time (top panel) and in terms of flash intensity (bottom panel). The solid lines represent all CG flashes, whereas shading shows the number of CG flashes which were time-correlated (< 1 s) with VLF events.

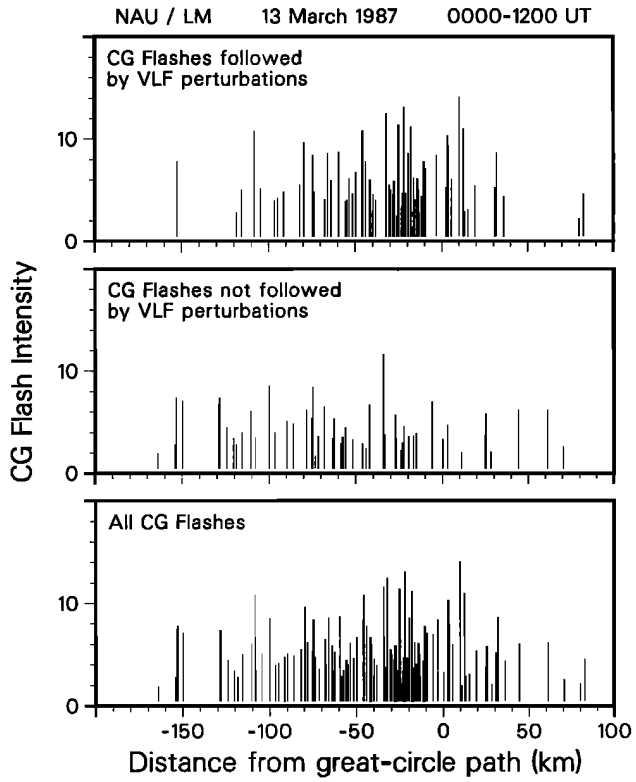

Fig. 8. The distribution of CG flashes in terms of flash intensity (with 1000 corresponding to a peak current of 200 kA) and distance from the NAU-LM path. The bottom panel shows all CG flashes detected by the network during the 0000-1200 UT period. The top panel shows the CG flashes that were time-correlated (< 1 s) with VLF perturbation onsets. The middle panel shows the distribution of CG flashes that were not accompanied by detectable (> 1%) VLF amplitude changes.

VLF events was accordingly smaller, and the three most prominent events were time-correlated with CG flashes.

Figure 4 shows that many CG flashes were time correlated with VLF perturbation onsets (there were also many VLF events for which no CG flash was detected and vice versa). The time correlations might be attributed to coincident alignment between two independent time series within the ~ 10-s resolution of the display, but high-time-resolution analysis presented in the following section indicates that in all cases the correlated CG flashes preceded the VLF event onsets by < 1 s. Such a circumstance is unlikely to occur between two independent time series (given that the rate of event occurrence in both time series is $\leq$ 40 events per hour) and by itself suggests a physical relationship between CG lightning and VLF perturbations.

For statistical purposes, CG flashes and VLF events were taken to be correlated only when the former occurred within < 1 s of the onset of the VLF perturbation. Figure 6 shows, on an hourly basis, the distribution of VLF events in terms of time (above) and event size, with shading indicating those events that were time-correlated with CG flashes. Figure 7 presents, again on an hourly basis, the distribution of CG flashes in terms of time (above) and flash size.

The distribution in terms of intensity and distance from the NAU-LM path of individual CG flashes is presented in Figure 8, where the distribution of those CG flashes followed by VLF perturbations are separately shown. Note that some of the statistics given earlier in Figures 6 and 7 as well as that given later in Figure 9 were derived from the data base of Figure 8.

Figure 6 shows that only ~ 50% of the observed VLF events were < 1-s time-correlated with CG flashes. This result is consistent with the fact that the CG flashes are only a subset of lightning discharges that occur within a storm center, intracloud discharges being generally more common [*Prentice and Mackeras*, 1977]. Furthermore, as many as 30% of the CG flashes may be missed by the lightning network within the coverage area shown by the circles in Figure 2. Outside the coverage area, lightning CG flashes are detected, but the percentage of missed flashes increases. Analysis presented in the next section supports these explanations, indicating that radio atmospherics recorded at Lake Mistissini (generated by CG as well as IC lightning) were time-correlated with a much larger percentage (~ 98%) of the VLF events.

The hourly percentage of detected CG flashes with accompanying VLF events ranged from 15% to 100% during the course of the 0000-1000 UT period. The percentage of correlated CG flashes during the prime period of VLF activity, i.e., 0400-0500 UT, was higher than during adjacent periods; on the other hand, during 0800-0900 UT, when both VLF

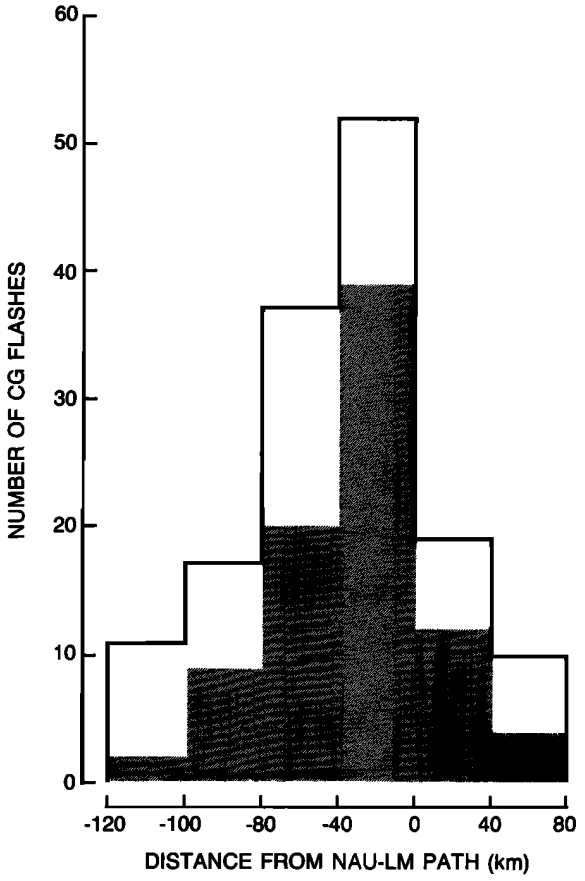

Fig. 9. Distribution of CG flashes in terms of distance of flash location from the NAU-LM great-circle path. The solid lines represent all CG flashes, whereas shading shows the number of CG flashes which were time-correlated (< 1 s) with VLF events.

and CG flash activity were reduced, all 6 of the CG flashes were time-correlated with VLF perturbations.

Figures 4 and 5 show that the intensity of the CG flashes was not well correlated with the size of the VLF perturbation. However, Figure 7 indicates that there was a tendency for a higher percentage of the larger flashes to be correlated with VLF events. Compare, for example, 79% for > 1000 versus 67% for 500-1000 and 56% for 0-500. Assuming lightning-induced electron precipitation to be the basic process leading to the VLF perturbations, one would expect the perturbation size to be correlated with the radiated field intensity from the discharge at frequencies below ~6-kHz [*Chang and Inan*, 1985]. Previous work has shown the VLF perturbation size (in phase as well as amplitude) to be well correlated with the intensity (below ~6 kHz) of associated magnetospheric whistlers [*Carpenter and LaBelle*, 1982; *Inan and Carpenter*, 1986]. The lack of a tighter correlation between the CG flash intensity (representing peak current in the first return stroke) and the VLF perturbation size in the present data set is not surprising, since the relationship between the peak current in the first stroke and the < 6 kHz radio energy that couples into the magnetosphere is not likely to be one-to-one. The fact that the resultant < 6 kHz radio energy (for a given total flash current) may be highly variable may also be the reason why some intense CG flashes located within 50-100 km of the path are not associated with VLF perturbations (see Figure 8).

Another question of general interest is the relative efficiency of positive versus negative CG flashes in producing VLF perturbations. In general, positive flashes (positive charge lowered to ground) are expected to be more effective simple because they are, on the average, more energetic [*Orville et al.*, 1987]. To investigate whether the sign of the charge lowered to the ground may somehow be important, we need to compare the response from negative and positive flashes of similar intensity. The data in hand are not sufficient to investigate this question, due to the very small number of negative flashes. Comparing the categories of 0 to 500 versus −500 to 0 from Figure 7, we see that 56% of the positive flashes are accompanied by VLF events versus 22% of the negative flashes. However, more data are clearly needed before we can infer definite conclusions along these lines.

Location of CG Flashes With Respect to the NAU-LM Path

The fact that the thunderstorm activity on March 13, 1987, was confined to within ±150 km of the NAU-LM path is likely to be significant. The sequence of VLF events observed on March 13, 1987, represents by far the most prominent VLF activity observed on NAU signal at LM during the November 1986–May 1987 period. The rate of event occurrence at times reached ~ 40 events per hour on March 13, while in most other cases only a few events per hour were detected (occurrence statistics on the NAU-LM path are discussed in a separate paper [*Inan et al.*, 1988]). The size of the VLF perturbations observed on this day was at times as large as 10-30%, whereas ~ 5% perturbations are typical. That the lightning activity is localized to within ±150 km of the NAU-LM path on this one day of unusually prominent observed activity suggests that (1) the spatial size of the perturbed ionospheric region(s) may be confined to the vicinity (±150 km) of the lightning discharges, and that (2) in the case of disturbances occurring midway along the NAU-LM path, amplitude changes may be most sensitive to perturbations occurring within ~ 150 km of the path, consistent with theoretical calculations of scattering from off-great-circle precipitation regions by *Wait* [1964].

On the other hand, the possibility that lightning is coincidentally localized on the path during this period of most outstanding VLF activity cannot be ruled out without a comprehensive joint analysis of the VLF data with that from the lightning network. For example, it is necessary to determine whether absence of outstanding VLF activity on other days (during the 7-month period mentioned above) is indeed associated with absence of localized activity near the NAU-LM path. Such an analysis is beyond the scope of the present paper. However, we can explore the spatial distribution question somewhat further by investigating whether the VLF event occurrence and/or characteristics are influenced by the location of individual lightning flashes with respect to the great circle path.

Figure 9 shows the distribution of CG flashes categorized in terms of distance from the NAU-LM path. The distribution of those flashes that are associated with VLF events is separately indicated by shading. Considering only those flashes to the west of the NAU-LM path (i.e., those for which the distance from the path is negative), we note that 75% of the CG flashes within 40 km are associated with VLF events as opposed to 54% and 53%, respectively, for those that lie at a distance of 40-80 km and 80-100 km from the path. This result suggests that the CG flashes closer to the path may be more effective in producing VLF events, and is thus consistent with the perturbed ionospheric regions being confined to the vicinity (±50-100 km) of the lightning discharges.

Although considerably fewer number of CG flashes have occurred to the east of the NAU-LM path, the distribution of these flashes (those for which the distance from path is positive as shown in Figure 9) shows a similar result; 63% of the CG flashes within 0-40 km of the path are followed by VLF events, as opposed to 40% of those within 40-80 km.

At first thought, this result might be expected to be a manifestation of the location of the storm center being near the NAU-LM path, thus leading to more intense flashes occurring closer to the path with lower intensity lightning activity at the edges. However, the data shown in Figure 8 indicates that the flash intensity is not the only controlling factor, since many larger intensity CG flashes within 50 km of the path are not associated with VLF events while lower intensity flashes at distances >100 km are followed by VLF perturbations.

The arguments presented above indicate that the March 13, 1987 data are consistent with the perturbed ionospheric regions being relatively small, confined near (±50-100 km) the lightning flash. However, it is clear that a definitive conclusion about the spatial distribution of lightning-associated ionospheric perturbation regions must await the study of cases where the lightning would be distributed over a much wider region than just ±150 km around the great circle path as was the case on March 13, 1987. It would also be desirable to compare only strokes of nearly equal intensity, although this may not be possible, since a statistically significant number of comparable size flashes occurring over a 3-6 hour period would be needed.

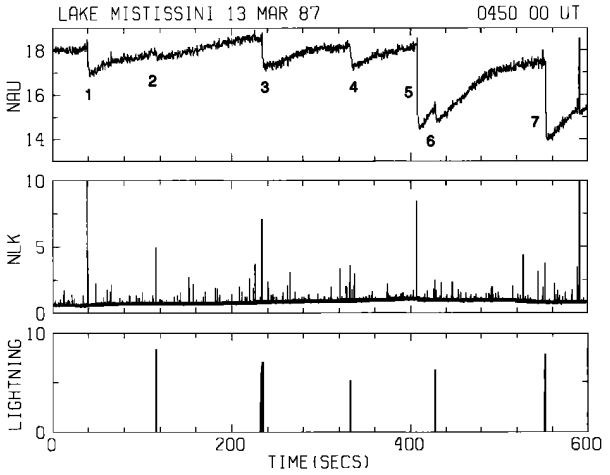

Fig. 10. Comparison of VLF events observed at LM on the 28.5-kHz NAU signal with radio atmospherics detected at LM on the 24.8-kHz NLK channel and cloud-to-ground (CG) lightning observed by the lightning network during 0450-0500 UT. The top panel shows the NAU signal intensity in the same format as Figure 4 except that the signal were time-averaged over only 0.64 s. The middle panel shows the signal intensity in a $\sim$ 300-Hz bandwidth centered at 24.8 kHz, the operating frequency of the NLK transmitter in Jim Creek, Washington. Since the NLK signal intensity is relatively low, radio atmospherics, generated by CG and/or intracloud lightning (or possibly some CG lightning missed by the network), are readily detected as sharp spikes. The NLK data shown were time-averaged over only 100 ms, so as to resolve the occurrence time of the spherics. The base level at arbitrary units of $A \simeq 1$ represents the NLK signal level. A cluster of very intense spherics (not detected by the network) occurring at $\sim$ 590 s is observed in the 28.5-kHz channel in spite of the 0.64-s averaging and is associated with a relatively small VLF event (signal level change). The lower panel shows the time of occurrence (with 1-s resolution) and intensity where 10 corresponds to a peak current of 200 kA for CG flashes detected by the SUNY-Albany network. The time $t = 0$ corresponds to the UT given in the upper right corner. The UT time is accurate to within $< \pm 10$ ms. The VLF events numbered 1 through 7 are later shown on expanded scale in Figure 14.

VLF Radio Atmospherics

Radio atmospherics generated by all lightning flashes (CG or intracloud) and detected with the Stanford VLF receivers at Lake Mistissini provide a way to further investigate the association with lightning of the VLF perturbation events. (Note that while the SUNY-Albany network excludes intracloud flash occurrences in the course of normal operations, the Stanford system records all spheric activity without discrimination.) At a location such as Lake Mistissini, Quebec, spherics from thunderstorm activity all around the world are received, and it is often difficult to identify particular spherics. However, in the case of March 13, 1987, with an isolated storm center within $\sim$ 1600 km of LM, it was possible uniquely to identify the spherics associated with the VLF events.

Two methods were used to detect the spherics. One employs the broadband VLF receiver, which was operated in a synoptic (1 min out of every 5) mode and therefore was useful for only a small subset of events. The second method utilizes the narrowband VLF channels, which were tuned to VLF transmitter frequencies and were operated continuously. Depending on the transmitter signal level in the 300-Hz-wide receiver bands, the more intense spherics are generally recognizable as short (< 50 ms) spikes at the receiver output. The 24.8-kHz NLK channel was used; this signal, originating in Jim Creek, Washington, was relatively weak as observed at LM, so that spherics were more easily recognized in the presence of the transmitter signal.

Figure 10 shows the activity during 0450-0500 UT, with the NAU amplitude in the upper panel, the NLK (24.8 kHz) receiver output in the middle panel, showing atmospherics, and the CG lightning data from the SUNY-Albany network in the lower panel. The correlation between the VLF events and the larger radio atmospherics is remarkable. Events such as those at $\sim$0450:40 UT (event 1) and at $\sim$0456:50 UT (event 5) that did not have accompanying CG flashes are coincident with large spherics that are likely to have been due to intracloud flashes or to missed CG flashes. Spherics are also clearly seen for the events that are coincident with CG flashes, although in some cases the spheric intensity in the 24.8 kHz band is relatively small. This result is not surprising; the CG flash intensity is a measure of the total flash current, whereas the power spectral density in any given narrow frequency range (24.8$\pm$0.15 kHz), would be expected to vary from one event to another.

Another sequence of large, well-defined VLF events is shown in Figure 11. Again there is a clear association between VLF perturbation events and spherics in the NLK channel. As shown later in Figure 15, this time correlation holds true to the point of there being a spheric preceding each VLF event onset by < 1 s. Events for which no CG flash was detected (such as events 6 and 7) are accompanied by clear spherics; in the case of the very last event in Figure 11, two spherics occurred in close succession and the corresponding step in the onset of the perturbation of the NAU signal can be seen. A similar circumstance occurred for the event at $\sim$0523:31 UT (event 2); multiple spherics were observed with even closer spacing.

Many spherics in Figure 11 do not have corresponding VLF events, as expected, since spherics observed at LM are due to lightning occurring on a very large scale. Neverthe-

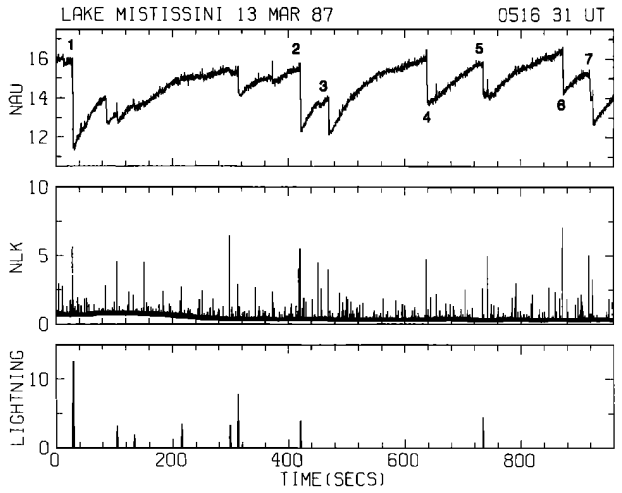

Fig. 11. Comparison of VLF events with radio atmospherics detected with the VLF receiver and cloud-to-ground (CG) lightning observed by the network during 0516:31-0531:31 UT. The format of the figure is identical to that of Figure 10. Events numbered 1 through 7 are later shown on an expanded scale in Figure 16.

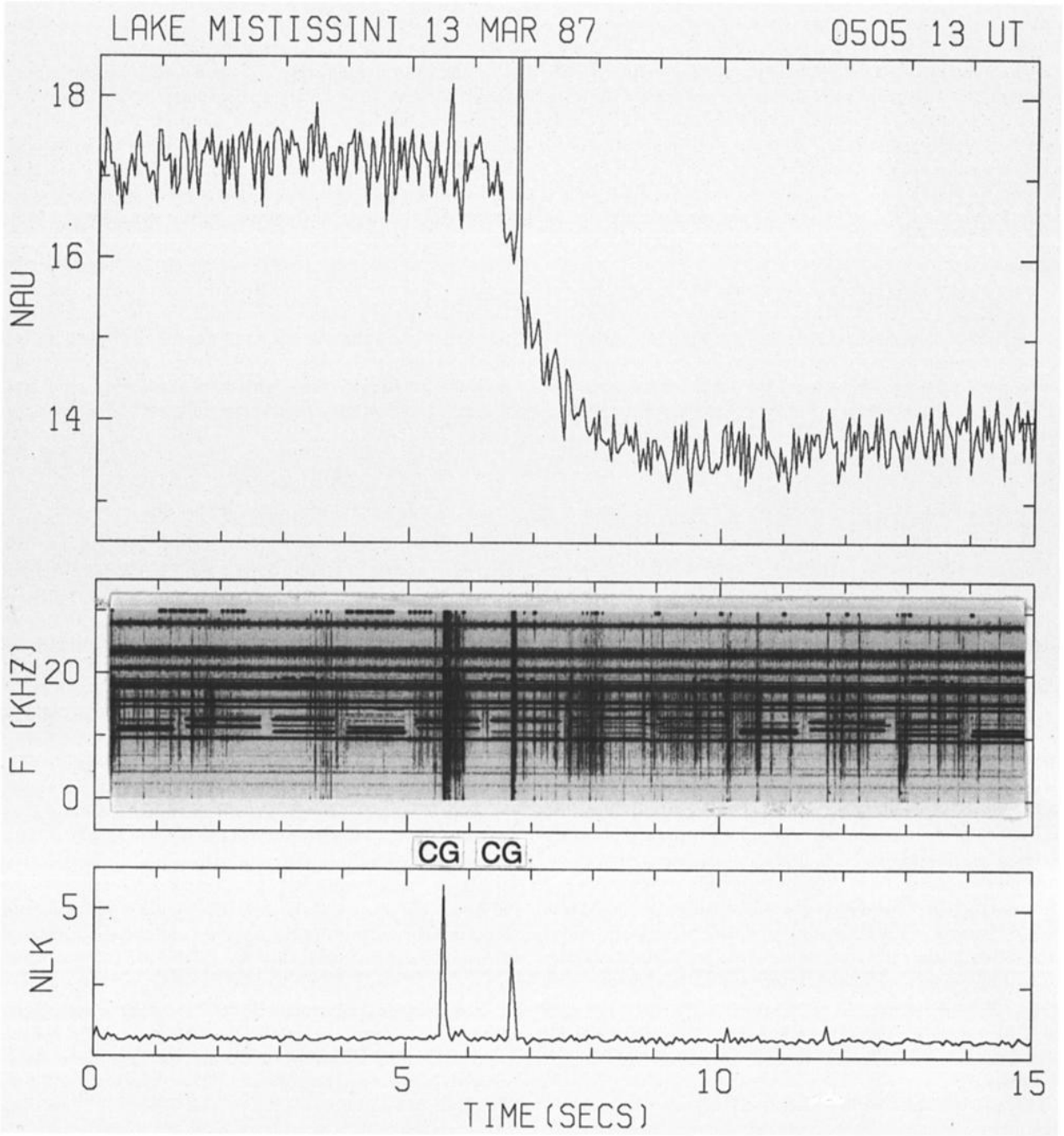

Fig. 12. VLF event observed at ~0505:18 UT in association with two successive intense spherics. The top panel shows the NAU signal amplitude in the same format as in Figure 10 but time-averaged over 80 ms. The middle panel shows the dynamic spectrum in the 0-30 kHz range as measured with the broadband VLF receiver operating in the synoptic mode for 1 min out of every 5. Omega navigation transmitter signals are seen as ~ 1-s-long pulses in the ~ 10 – 14 kHz range. Other VLF transmitters, operating with continuous modulations are apparent in the 15-30 kHz range, including the NAU signal at 28.5 kHz. The vertical lines on the spectrum are impulsive spherics generated by CG and/or intracloud lightning. The lower panel shows the signal intensity in the NLK channel as described for Figure 10. The two intense spherics are clearly visible, but weaker spherics, observed in the broadband receiver, are not detectable in the NLK channel. The seconds during which a CG flash was detected by the SUNY-Albany network are indicated; they correspond to the two intense spheric clusters seen in the middle panel. The time $t = 0$ corresponds to the UT given in the upper right corner.

less, for the case shown, most of the stronger spherics were associated with VLF events, probably because of the isolated nature of the storm center and its relative proximity to LM.

To confirm the utility of the NLK channel for detecting spherics, we show in Figure 12 an event observed during one of the synoptic 1-min broadband VLF recording periods. Here the middle panel shows the 0-30 kHz broadband spectra, clearly illustrating two intense spherics arriving within ~ 1-s of one another. (The NAU amplitude goes off scale

at the time of the second spheric.) The top panel shows the associated VLF event and the lower panel the spheric intensities in the 24.8±0.15 kHz band as measured with the NLK receiver. High-resolution temporal features of the VLF events (such as the ~ 0.6-s delay between spheric and event onset) are clearly evident in Figure 12. These are discussed below in a separate section.

Figure 13 shows a sequence of two successive VLF events in the format of Figure 12. In these cases, some of the weaker spherics are also detected as smaller spikes in the NLK channel.

No whistlers were detected in synoptic LM records such as those of Figures 12 and 13. However, in the course of the 12-hour period of observations on March 13, 1987 160 out of 163 VLF events were found to be accompanied by atmospherics time coincident to within ~ 1 s of the VLF perturbation onset. Such a time correlation confirms a causative connection between lightning-induced spherics and observed VLF/LF perturbations, in spite of the lack of recorded information about the magnetospherically propagated wave.

Cloud-to-Ground (CG) Versus Intracloud (IC) Lightning

The fact that nearly all of the observed VLF perturbations were time-correlated with strong spherics (that stand out among others) indicates that the events were caused by lightning occurring in the localized storm center shown in Figure 3. That only ~ 50% of the VLF events were time correlated with CG flashes detected by the network suggests that at least some of the IC flashes witin the same storm system may have also produced the VLF events. An alternative explanation would be that all of the remaining 50% of the VLF perturbations were caused by CG flashes that were missed by the network. The localized storm on March 13, 1987, was at the edge of the primary coverage circles given in Figure 2. The detection efficiency of the network may decrease to ~ 50% outside this region. On the other hand, it is known that flash intensities in the March 13, 1987, storm were unusually high and that there is less attenuation of the lightning signal over the relatively higher conducting seawater. These factors would tend to increase the detection efficiency. In view of these considerations, we can only conclude that we do not know the detection efficiency of the network for flashes occurring far out in the Atlantic.

The question of whether intracloud flashes can produce whistlers (and thus whistler-induced electron precipitation leading to ionospheric perturbations) is an interesting one. Experimental data (ground-based measurements) indicates that the IC flash is not a strong source of radiation in the 3-10 kHz range and that the radiated field intensity for a CG flash can be 10-20 times higher than that for an IC flash [*Brook and Ogawa*, 1977]. However, this difference might be compensated by the fact that the radiation pattern of an IC flash (with main lobe pointed upward) would lead to more favorable excitation of overhead magnetospheric paths.

Other related data support our hypothesis that a significant fraction of the remaining ~ 50% of the VLF perturbations were possibly caused by IC flashes. In recent work involving joint analysis of whistler data with SUNY-Albany data on CG lightning, D. L. Carpenter and R. E. Orville (manuscript in preparation, 1988) find that the detected CG lightning accounts for only ~ 50% of the observed whistlers. (In those cases analyzed, the lightning was located well within the coverage circles shown in Figure 2 so that the detection efficiency of the network can be expected to be at least 70%.) Since most measurable characteristics of the whistlers (dispersion, multiplicity of traces, and frequency range) associated with CG lightning were similar to nearby whistlers without a detected CG flash, Carpenter and Orville concluded that IC flashes within the same storm center are the most likely source of the remaining ~ 50% of the observed whistlers.

In light of the above, our observations on March 13, 1987, suggest that IC flashes within the same storm center may have produced a significant number of the observed VLF perturbations. Further data are needed, however, to more firmly establish this connection. In particular, it would be desirable to analyze cases where a similarly localized storm is located well within the coverage of the SUNY-Albany network.

4. High Resolution Analysis of Temporal Signatures

Figure 14 presents high time resolution displays of all of the VLF events observed during the 0450–0500 UT period illustrated in Figure 9. For each event, data over a 10-s period centered on the event onset are shown. The top panels display the 28.5-kHz NAU signal amplitude, whereas the lower panels show spheric information from the 24.8-kHz NLK channel. The 1-s period during which a CG flash was detected by the SUNY-Albany network is indicated for some of the events; no CG flash was detected for the others.

Some of the events in Figure 14 are better defined than others and the temporal signatures are variable. However, a number of consistent features become apparent upon analysis. For all cases the 24.8-kHz NLK records reveal an atmospheric preceding the event onsets by < 1 s. In fact, with the resolution shown, many of the spherics were intense enough to be visible on top of the 28.5-kHz signal itself, sometimes momentarily saturating the receiver and causing a sharp decrease in output (as in the case of the event 7 at 0459:08 UT).

The best defined events at 0456:43 UT (event 5) and 0459:08 UT (event 7) exhibit a delay of ~ 0.6 s between the spheric and the event onset, and an onset duration (as measured between the 10% and 90% points) of ~0.5-1.0 s. The time of event onset is not as well defined in some of the other events, although a delay of ~ 0.6-s is evident. The duration of onset seems at first to be rather variable, as in the case of events 1, 3, and 4, respectively, at 0450:35, 0453:49 and 0455:29 UT; however, this is likely to be due to multiple spherics, as evidenced in the lower panels of Figure 14. Event 3 at 0453:49 UT is a good example; the first spheric at ~ 0453:53 UT starts an event which then appears to be prolonged by another event induced by the spheric at ~0453:54 UT.

In the case of event 1 at 0450:35 UT, a possibly causative spheric is evident at 0450:37, superimposed on the 28.5-kHz signal, but is not seen on the 24.8-kHz NLK channel. This circumstance is likely to occur on occasion, since, as mentioned above, the spheric intensity in the narrow band of 24.8±0.15 kHz is likely to be variable. To further illustrate, this event is shown in Figure 15 in the format used for Figures 12 and 13. A number of weaker spherics are evident

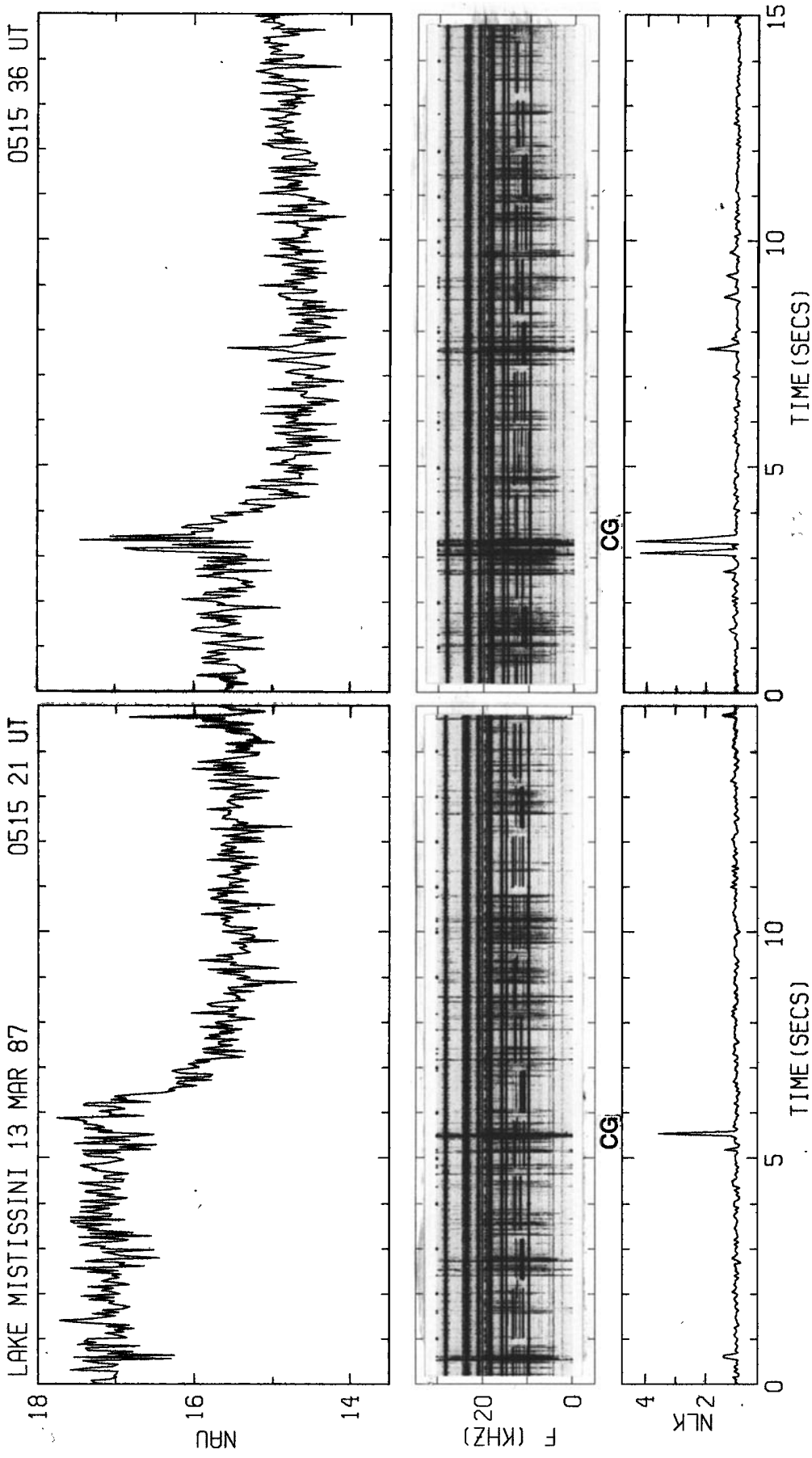

Fig. 13. Two successive VLF events observed in association with intense spherics. The second event seems to be associated with a closely spaced pair of spherics. The format of this figure is similar to that of Figure 12.

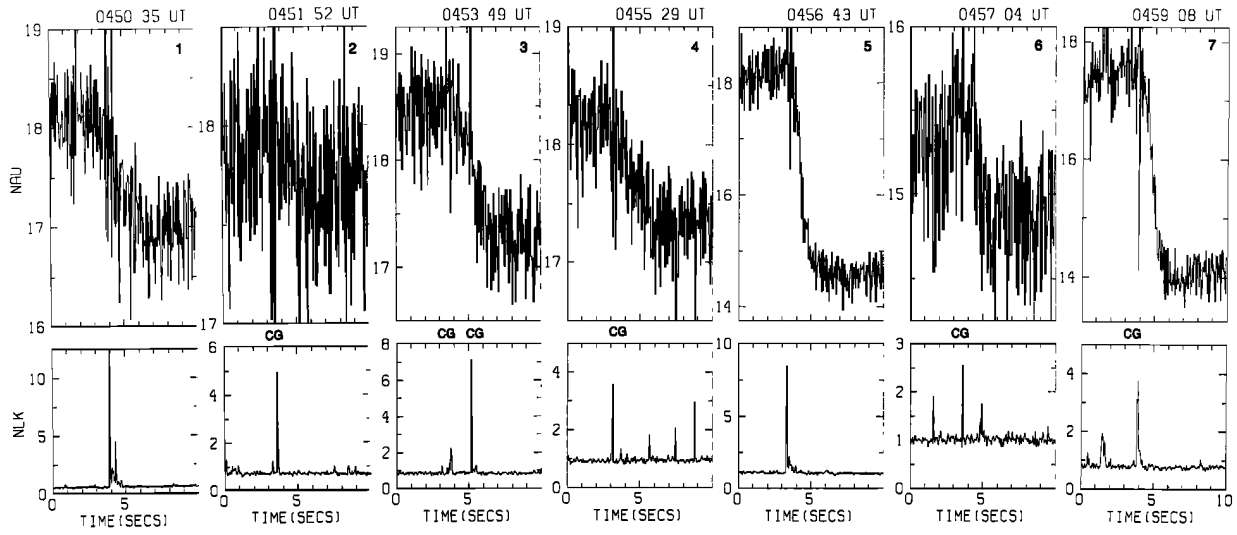

Fig. 14. High-resolution display of the VLF events observed during 0450-0500 UT (Figure 10) together with spherics detected in the NLK channel. For each event, enumerated as 1 through 7 in Figure 10, a 10-s period roughly centered on the event onset is shown, with time $t = 0$ corresponding to the UT given in the upper right corner. The top panels show the NAU signal intensity time-averaged over 40 ms. The vertical axis shows signal strength (A) in linear arbitrary units, with $A = 0$ representing the absence of signal. The lower panel shows signal intensity in the 24.8-kHz channel time-averaged over 50 ms. Different amplitude scales are used for each event. The 1-s periods during which a network CG flash were detected are so indicated.

in the broadband data, including one at 0450:37 UT ($t \simeq 8$ s in Figure 15); however, it is not clear why this particular spheric should have been causative of the VLF perturbation. No network CG flash was detected during this 10-s period. It is possible that the lightning intiating this event was a particular type of intracloud discharge that radiates a relatively small amount of energy into the Earth-ionosphere waveguide. We note that this event is one of only three VLF events out of 163 which were not preceded with a causative spheric as detected on the NLK channel. It is also possible that the VLF perturbation is due to lightning discharges in another (far away) storm center or due to other causes unrelated to lightning.

Figure 16 shows a better defined set of events with relatively larger amplitude changes observed during 0516-0532 UT. These events are displayed on a compressed scale in Figure 10. A spheric consistently precedes the event onset by ~ 0.6 s, and the onset duration for all of the events shown is < 1 s.

Gyroresonant Whistler-Particle Interaction in the Magnetosphere

The event signatures illustrated above, in particular (1) the ~0.6-s delay between the causative spheric and the VLF event onset and (2) the < 1-s duration of the event onset, are generally consistent with the predicted signatures of lightning-induced electron precipitation (LEP) events resulting from gyroresonant interactions in the magnetosphere between energetic (> 40 keV) particles and the whistler waves [*Chang and Inan*, 1985].

Considering an average model of magnetospheric cold plasma density inside the plasmasphere, *Chang and Inan* [1985] have quantitatively estimated the time profile and energy content of precipitation fluxes that would be induced by lightning-generated whistlers at typical frequencies of > 500 Hz and propagating in field aligned ducts over a range of L shells. For equatorial cold plasma density at $L \simeq 2.5$ of $n_{eq} \simeq 1000$ cm^{-3}, the arrival time at the ionosphere of the onset of the LEP pulse was estimated to be ~ 0.3 s, and the duration of the LEP pulse was found to be ~ 0.5 s. Both of these quantities are dependent on the cold plasma density, the assumed energy spectrum of the trapped particle distribution, and the whistler frequency spectrum. Furthermore, somewhat longer delays would be expected if the causative whistler propagated in the nonducted mode. In view of these factors, the measured event signatures fall within the range predicted by the gyroresonance model. This result supports the hypothesis that the observed VLF events are ionospheric signatures of LEP events induced during whistler-particle gyroresonance interactions in the magnetosphere.

VLF Events With Very Rapid Signatures

Signatures of perturbation events observed before ~ 0130 UT differed from those occurring later in a number of respects. In this period perturbations with rapid onset and slow decay as defined above were positive amplitude changes (see Figure 5), as opposed to negative changes observed during most of the rest of the 12-hour period. The associated lightning was in the same general area, but in these cases may have produced a different type of ionospheric response, one more strongly affecting Earth-ionosphere waveguide modal relationships than simply causative of wave absorption, and thus consistent with the occurrence of signal enhancements. The observation of both positive and negative changes on the same signal during the night is not in itself surprising, in view of previous reports of such changes, sometimes alternating over the course of minutes [*Carpenter and LaBelle*, 1982; *Carpenter and Inan*, 1987]. How-

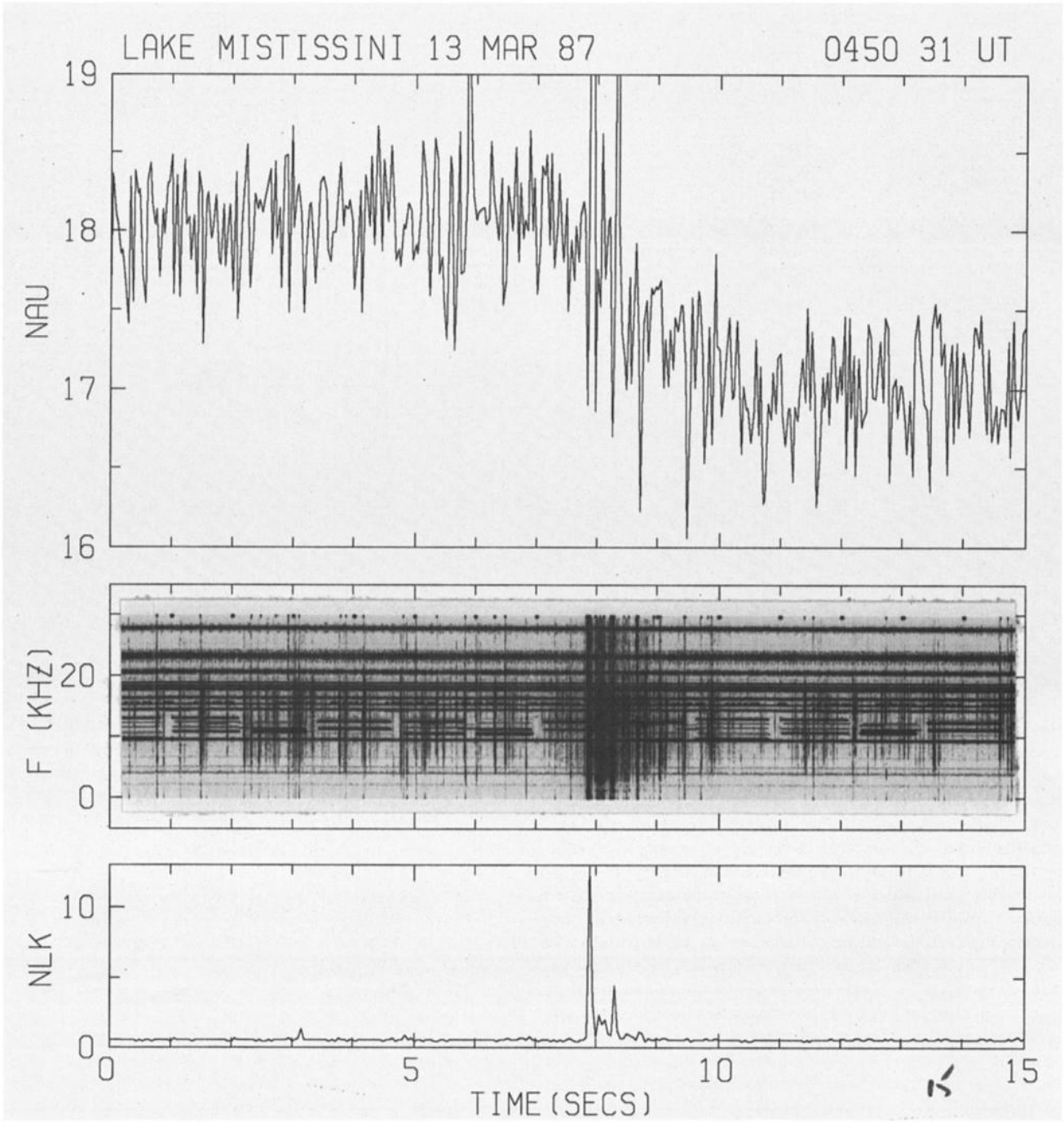

Fig. 15. Expanded record of the first event from Figure 14 shown in the format of Figure 12, together with the 0-30 kHz broadband spectrum.

ever, when the events are examined in high time resolution, a number of unusual features appear. Figure 17 shows six of the signatures, centered within 200-s time segments. Instead of decaying after a fast change toward the initial unperturbed level (as in Figures 10 and 11), the entire signal level appears to shift upward, and any distinctive decay process is masked by a continuing oscillatory pattern of the background signal. Additional differences are shown in the high-time-resolution display of Figure 18. As in the case of the negative changes shown in Figures 14 and 16, a spheric is observed in the NLK channel in time correlation with each of these positive events. However, in the cases shown in Figure 18 there seems to be virtually no delay between the spheric and the onset of the perturbation. The data illustrated were recorded on tape at a rate of 50 Hz, and are presented in Figure 18 with 40-ms averaging. Thus any delays between the spheric and perturbation onset must be < 50 ms.

The duration of the event onset (i.e., rise time) seems to be highly variable, being in the range of 1-2 s for most events shown. However, for the first event at 0007:22 UT, the rise time seems to be < 50 ms.

Perturbation events with rise times of < 50 ms were observed previously at Siple Station, Antarctica ($L \simeq 4.3$), together with a magnetospheric whistler and a causative

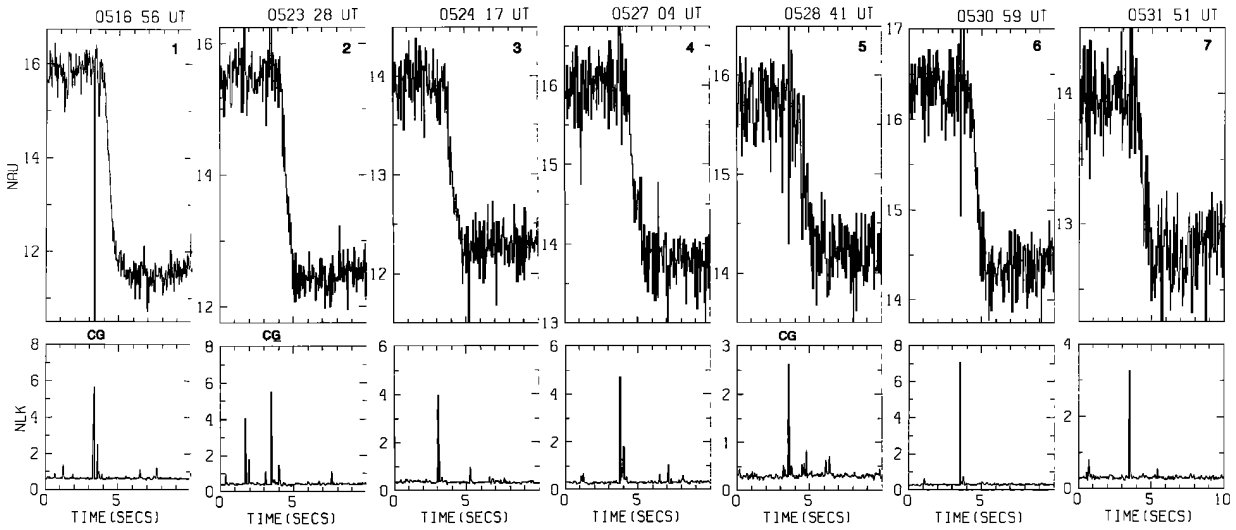

Fig. 16. High-resolution display of some of the VLF events observed during 0516:31-0531:31 UT (Figure 11) together with spherics detected in the NLK channel. The format of this figure is identical to that of Figure 14. Only selected events, enumerated from 1 through 7 in Figure 11, are shown.

spheric that appeared to be within 50 ms of event onset [*Armstrong*, 1983]. It is not clear how those events are related to the present data, since, for example, the Antarctic cases were interpreted in terms of perturbations induced near the NSS transmitter, and thus near the beginning of a $\sim 10,000$-km-long signal path. However, in neither case are the event signatures consistent with the equatorial gyroresonance model. Instead these events imply that there exists a more direct coupling mechanism between the lightning discharge and the ionospheric D region. One possible mechanism suggested for such events involves whistler-particle resonant interactions occurring in the topside ionosphere [*Neubert et al.*, 1987]. It might be possible that some type of scattering interaction at low altitudes near the particle mirror points occurs as the result of the presence of large transient electric fields from lightning [*Kelley et al.*, 1985; *Goldberg et al.*, 1987]. An even more direct mechanism may exist; recent observations of "synchronized" whistlers and possible triggering of lightning from the magnetosphere [*Armstrong*, 1987] suggest that there may exist some form of direct coupling between cloud tops and ionization enhancements in the bottomside ionosphere, perhaps involving upward discharges.

The reason for the occurrence of the "early" VLF events in the first $\sim 1\frac{1}{2}$ hours of the 12-hour sequence is not known. The rate of occurrence and location and/or size of the lightning flashes do not seem to be recognizably different during this period as compared to the later periods. This may imply that a magnetospheric effect (such as particle injection or availability of whistler propagation paths), or an ionospheric or mesospheric local time effect (such as the variation of background ionization during the night) may play an important role. It is also possible that the lightning activity during this period played a role in establishing the ionospheric/magnetospheric propagation conditions (for example, by contributing to the formation of "ducts") that facilitated the large number of events observed in the following hours. Formation of field-aligned irregularities by thundercloud electricity was previously suggested by *Park and Helliwell*, [1971].

5. Multiple Signal Measurements: VLF/LF "Imaging" of LEP Region(s)?

Up to now we have discussed only VLF events on the 28.5-kHz NAU signal observed at Lake Mistissini. As mentioned in connection with Figure 5, the normal mode of operation of the Stanford experiment at Lake Mistissini involves simultaneous measurement of multiple subionospheric VLF/LF signals arriving on a number of paths. Such measurements are potentially important for extracting information on the spatial distribution of the perturbed ionospheric

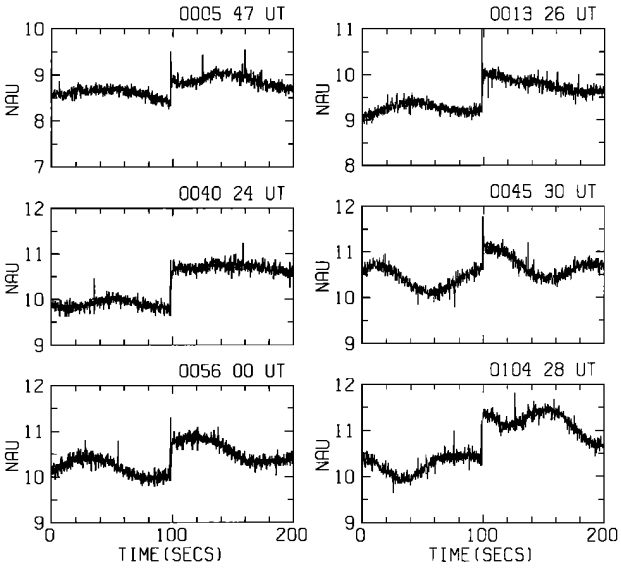

Fig. 17. Expanded record of the fast signal perturbations observed as signal increases (positive VLF perturbation events) during 0000-0100 UT. A 200-s period centered on each event onset is shown. The intensity (A) of the 28.5-kHz NAU signal is shown in linear arbitrary units, with $A = 0$ representing the absence of signal, as measured within a bandwidth of ~ 300 Hz and time-averaged over ~ 0.16 s.

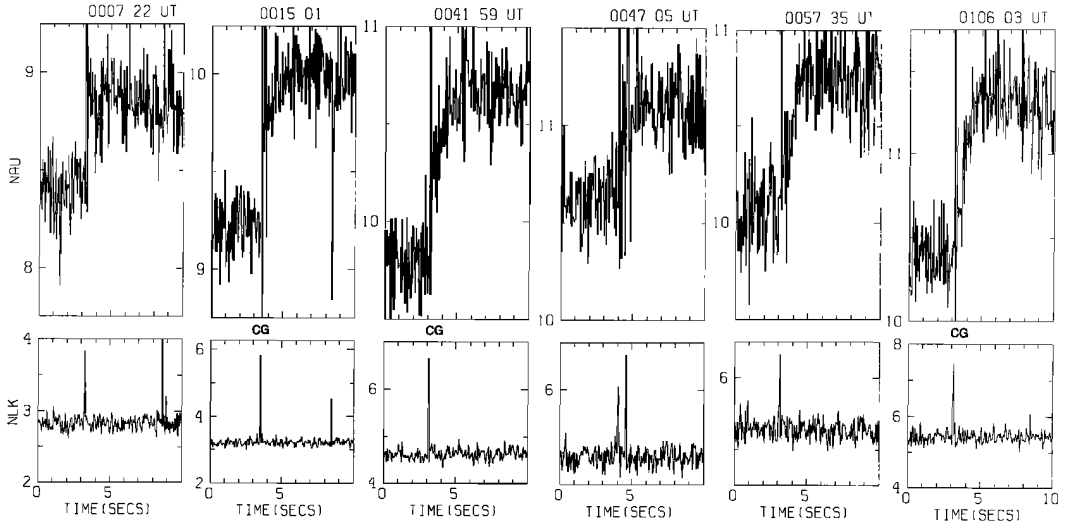

Fig. 18. High-resolution display of the fast positive VLF events observed during 0000-0130 UT (Figure 17) together with spherics detected in the NLK channel. The format of this figure is identical to that of Figure 14.

regions (i.e., electron precipitation region(s)), as previously suggested [*Inan and Carpenter*, 1987].

The path geometry and the observed amplitudes of four different signals during the 0500-0600 UT period are shown in Figure 19. The location of the CG lightning flashes detected by the SUNY-Albany network are indicated as pluses on the map. During the period of peak event activity on the 28.5-kHz NAU signal, the amplitudes of the 21.4-(NSS), 24.0-(NAA), and 48.5-kHz signals exhibited slow variations over time scales of a few minutes to tens of minutes. However, no evidence of VLF events (as defined by the characteristic rapid (< 1 s) onsets followed by slower decays) was seen on the NSS and 48.5-kHz signals. A few very small perturbations appear on the NAA signal; however, these generally represent amplitude changes smaller than 1%.

In the absence of the information on lightning location, multipath data such as that of Figure 19 could have been used to infer the existence of a precipitation region either at $L < 2.5$ and of unknown east-west extent, or possibly at $L > 2.5$ and of limited longitudinal extent. Observations at other sites of additional subionospheric paths, for example, south-going paths from the NAA transmitter and east-going paths from the NSS transmitter, would have permitted more refined estimates.

During the course of the 12-hour period on March 13, 1987, few simultaneous perturbations of NSS and NAU or

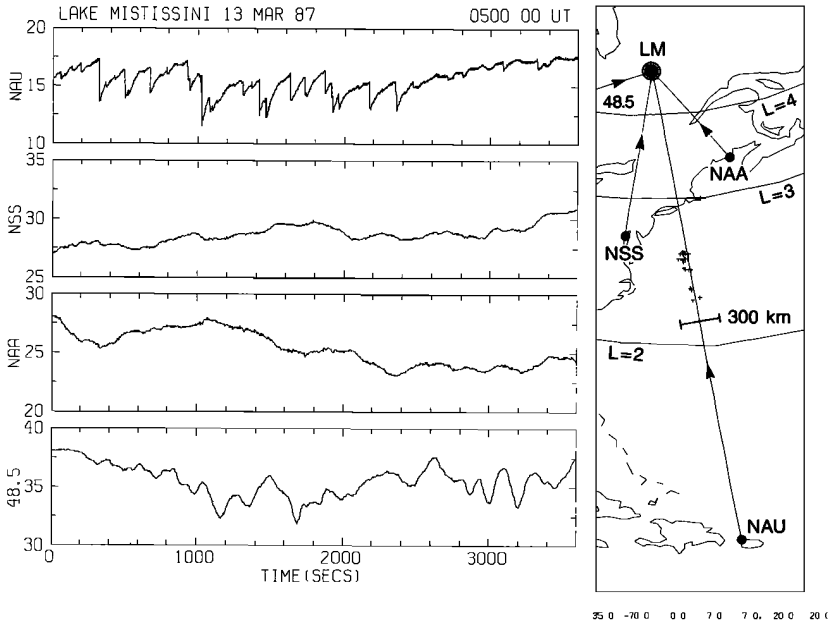

Fig. 19. Intensity variations of four different signals observed at Lake Mistissini during 0500-0600 UT. The great-circle propagation paths are shown on the right. The locations of CG lightning flashes detected during this period are shown on the map as pluses. The signal intensities were all measured within a ~ 300-Hz bandwidth and averaged over ~ 1 s. The transmitter frequencies are 28.5 (NAU), 21.4 (NSS), 24.0 (NAA) and 48.5 kHz.

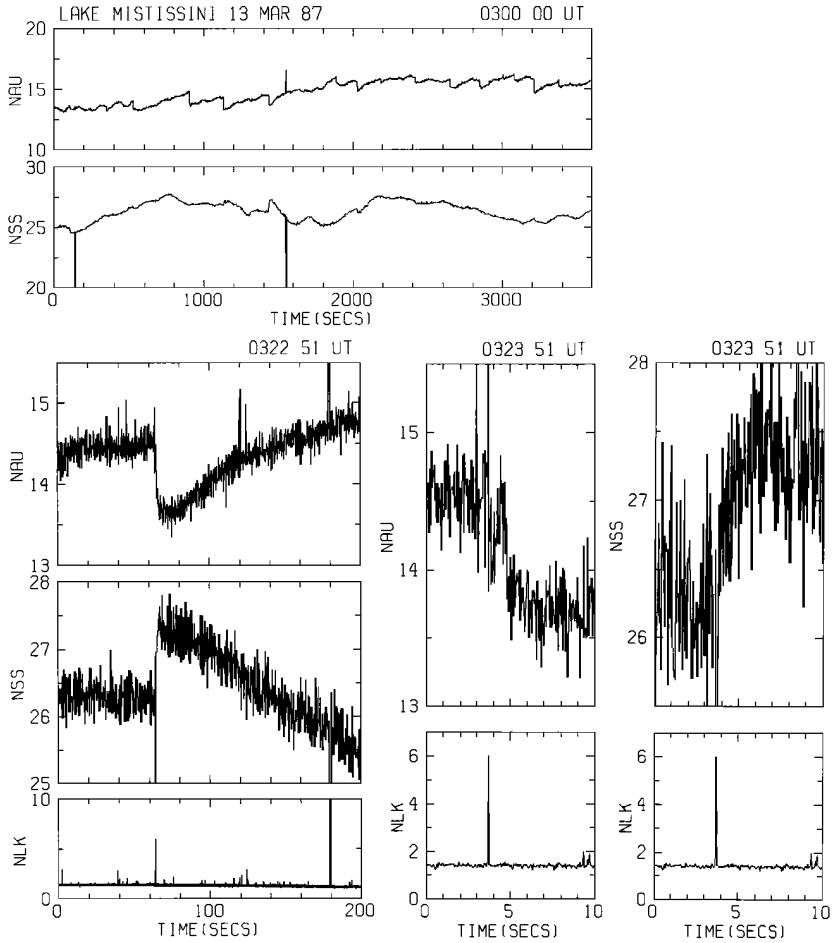

Fig. 20. Illustration of VLF perturbation events observed simultaneously on the NAU (28.5 kHz) and NSS (21.4 kHz) signals. The top two panels show the data during the 0300-0400 UT period. The lower left panels show one of the simultaneous events on an expanded scale, together with the asssociated spheric as detected in the NLK channel. The lower right panels show 10-s periods centered around the event onsets, in the same format as Figure 14. The UTs given on the upper right corners correspond to $t = 0$ on the horizontal axes. The corresponding great-circle propagation paths are displayed in Figure 19.

of NAA and NAU were observed. Figure 20 shows examples of the former during 0300-0400 UT. The top panels show the entire period. A number of events were observed on the NAU signal, three of which appear to be coincident with VLF events on NSS. Only the first of these three NSS events, one of the two smaller ones, was correlated with a detected CG flash (see Figure 4). The largest of the three events on NSS is shown in high-time resolution in the lower panels, with the corresponding NAU and NLK data. The NAU signature is similar to that of preceding and following NAU events that had no counterpart on NSS. The large isolated flash at $\sim$ 180 s on the lower left panels momentarily saturated the receiver channels, but did not seem to cause a VLF event. This flash, which was not registered by the SUNY-Albany network, may have been very close to the receiver, and hence poleward of the region within the plasmasphere ($L < 3$) favored for precipitation of $E > 40$ keV electrons.

The distribution of CG lightning activity for this period is shown on the 0300 UT panel of Figure 2. The lightning activity was slightly to the west of the NAU-LM paths, and therefore closer to NSS. That the causative flash in Figure 20 is interpreted as an IC discharge should also be noted, since the spatial extent of such flashes may well be as high as a few tens of kilometers. The simultaneous events observed on the NSS signal may have been due to excitation of ducted whistler paths with ionospheric projections near the NSS-LM path, or to the excitation of nonducted waves over unusually extensive regions regions by the few flashes in question. The latter situation might occur in the presence of higher than usual trapped particle fluxes, or stronger than usual excitation of whistler-mode waves at the frequencies of interest ($<\sim$ 6 kHz).

An interesting aspect of the data shown in Figure 20 is the apparent difference in the VLF signatures on the NSS and NAU signals. That the signal changes are of opposite polarity is attributable to the multiple mode nature of subionospheric VLF propagation [*Tolstoy et al.*, 1986]. The NAU signal perturbation onset is seen to occur $\sim$ 0.8 s after the radio atmospheric, consistent whistler-induced electron precipitation as discussed in the previous section. The high-resolution record of the NSS signal appears to show the event onset following the spheric with little delay, similar to the "fast" events observed during the first $1\frac{1}{2}$ hours of the observation period. However, we note that the NSS record is

highly fluctuating and it is difficult to determine the onset time without the benefit of repeated events.

6. DISCUSSION

The data reported above suggest an interpretive picture differing in important ways from that based on observations of VLF events in the southern hemisphere. The features of the present case such as activity duration and typical VLF event amplitude, in conjunction with the lightning location data, suggest that the precipitation region(s) affecting the NAU signal were centered within $\sim$ 150 km of the great-circle signal path. Further inferences are that the precipitation regions may have been of order 50-100 km in radius, and approximately centered on the causative flashes. This implies that the spatial distribution of waves injected into the magnetosphere depended strongly upon lightning location, and hence that the waves were nonducted. The presence of ducted propagation, with ionospheric projections near the NAU signal path, cannot be ruled out, but the apparent fall-off in event occurrence with relatively small changes in source distance from the great circle path, the lack of correlation between lightning intensity and VLF event amplitude, and the lack of two-hop whistlers observed in the synoptic broadband records at LM (Figures 12, 13, 15) are also not supportive of a ducted-wave interpretation. (The fact that the temporal signatures exhibited by the nonducted events are within the range of the predictions of a gyroresonant scattering model based on ducted propagation [i.e., *Chang and Inan*, 1985] may be due to the fact that, at $L \simeq 2.5$, the half-hop time delay from the ground to the equator for and nonducted waves is only slightly larger than that for ducted waves and also the fact that the resonant particle energies are similar [*Inan et al.*, 1985*b*].)

In contrast, southern hemisphere ground data have been interpreted as indicative of the occurrence of precipitation regions in the hemisphere opposite to that of the lightning source [e.g. *Leyser et al.*, 1984; *Carpenter et al.*, 1984]. Individual precipitation regions, while in some cases inferred to be of a size comparable to that reported above [*Carpenter and LaBelle*, 1982; *Inan and Carpenter*, 1987] and centered within 200 km of affected propagation paths [*Carpenter and LaBelle*, 1982], are not evidently confined to a narrow region magnetically conjugate to the ionosphere over the flash, but instead have been inferred to be either multiple in nature, or somehow sufficiently distributed to simultaneously affect paths spaced by distances of order 1000 km [*Leyser et al.*, 1984; *Carpenter and Inan*, 1987]. Persuasive, although not conclusive, evidence of an association of VLF events with ducted wave energy has been found [*Carpenter and LaBelle*, 1982; *Inan and Carpenter*, 1986].

The limited data from satellites support the underlying picture of a lightning-associated electron scattering process, but have yielded a still different picture in showing that precipitation regions may have a north-south extent of up to $\geq$ 500 km, based simply on the length of the orbital track over which events have been observed [*Voss et al.*, 1984].

The diversity of interpretations just described suggests that lightning associated supionospheric VLF perturbation phenomena are multifaceted; only particular aspects of it have been readily apparent in any one of the experiments thus far conducted. Consider also the observation of VLF perturbation events with a different signature during the first $\sim 1\frac{1}{2}$ hours of the 12-hour period discussed above. The lack of a $\sim$ 0.6-s onset delay and other differences from the later events suggest that near equatorial scattering interactions were not a major factor in these cases, and that a fundamentally different process coupling the lightning and lower ionosphere was probably involved.

7. SUMMARY

In an initial study of the relations between northern hemisphere lightning and amplitude changes observed on nearby subionospheric VLF signal paths, evidence has been found suggesting that lightning location can be a key factor in the burst particle precipitation that is inferred to cause the signal changes. On March 13, 1987, when an unusually well defined and long enduring set of changes was observed on a VLF signal path extending south to north off the east coast of the United States, an isolated thunderstorm center located within $\pm$150 km of the subionospheric great circle propagation path persisted for $\sim$ 12 hours. That the storm center was thus located in this case of unusually high activity (in terms of event size and rate) suggests that the ionospheric regions perturbed by lightning were localized to the storm electrical center. It also suggests that for this case of ionospheric perturbations midway along the south-north signal path, the subionospheric VLF signal amplitude was most sensitive to perturbations occurring within $\sim$ 150 km of the great-circle path.

The percentage of CG flashes that were accompanied by VLF perturbations increased with flash intensity as well as with decreasing distance between the flash location and the subionospheric great-circle propagation path. This result, summarized in Figure 9, is consistent with the ionospheric regions perturbed in individual events being of order 50-100 km in radius and centered near their causative flashes. However, an important limitation of our present data set was the fact that the thunderstorm was highly-localized and definitive conclusions concerning the spatial distribution of perturbed ionospheric regions must await the study of cases where the lightning is distributed over a much wider region.

Individual VLF amplitude perturbations (> 1% changes occurring within < 1 s) were consistently found to be time-correlated (< 1 s) with strong atmospherics that were also detected by the multichannel VLF receiver. A subset of these spherics was separately detected as cloud-to-ground flashes by the SUNY-Albany east-coast lightning detection network, in terms of their occurrence time as well as location. Only $\sim$ 50% of the VLF perturbations events were time-correlated with CG flashes, suggesting that intracloud (IC) lightning may have caused a significant number of the remaining VLF perturbations. However, the thunderstorm activity on this day was at the edge of the primary coverage regions of the lightning network and the possibility that most of the remaining $\sim$ 50% of the VLF events were due to CG flashes missed by the network cannot be ruled out.

The percentage of CG flashes that were accompanied by VLF events increased with flash intensity and decreased with distance from the NAU-LM path. The fact that some intense and nearby CG flashes did not produce detectable events is attributed to the variability of the radiated field intensity at frequencies of interest (i.e., < 6 kHz for whistler-particle interactions occurring at $L \simeq 2.5$).

The data were consistent with previously reported studies

from the conjugate region and satellite-based observations in that they support a high-altitude gyroresonance wave-particle scattering interaction as a basic element in the process leading to the signal perturbations. However, there appear to be significant differences from the other studies. For example, the important waves in the present study appear to have been those injected near the flash, while the evidence from the conjugate region emphasizes the role of waves that propagate in distributed regions, projections of which may in some cases extend of order 1000 km from the field lines passing near the flash.

A remarkable feature of the present study is the observation during the first $\sim 1\frac{1}{2}$ hours of the 12-hour nighttime period of VLF events with unusually early/fast temporal signatures. These events, which may be related to events previously found in Antarctic data, have now been found to be associated with specific CG lightning flashes located within $\sim$ 150 km of the affected signal path. It is therefore clear that lightning is capable of perturbing the nearby lower D region (sufficiently to affect VLF propagation) more or less immediately, within < 50 ms of the discharge. The physical mechanism of this type of fast troposphere-ionosphere coupling is under study. Further details of the early/fast events will be presented in a future report.

Acknowledgments. We thank our colleagues at the STAR Laboratory for many useful discussions, notably R. A. Helliwell and D. L. Carpenter. We are grateful to J. P. Katsufrakis for his direction of the Stanford field programs, including the establishment of the new station at Lake Mistissini (LM), Quebec, and his early recognition of the potential use of the NAU transmitter in Puerto Rico for subionospheric VLF/LF measurements. We thank T. Wolf and W. Burgess for their contributions to the acquisition and analysis of the LM Trimpi data and K. Fletcher for her help in typing this manuscript. The acquisition of broadband VLF data (Figures 12, 13 and 15) was supported by NSF contract DPP-83-17092 at Stanford University. This work was supported by NSF under contract ATM8415464 at Stanford University and ATM8703398 at SUNY.

The editor thanks R. H. Holzworth and M. J. Rycroft for their assistance in evaluating this paper.

REFERENCES

Armstrong, W. C., Recent advances from studies of the Trimpi effect, *Antarct. J., 18*, 281, 1983.

Armstrong, W. C., Lightning triggered from the Earth's magnetosphere as the source of synchronized whistlers, *Nature, 327*, 405, 1987.

Brook, M., and T. Ogawa, The cloud discharge, chap. 6, in *Lightning*, edited by R. H. Golde, Academic, San Diego, Calif., 1977.

Carpenter, D. L., and U. S. Inan, Seasonal, latitudinal and diurnal distributions of whistler-induced particle precipitation events, *J. Geophys. Res., 92*, 3429, 1987.

Carpenter, D. L., and J. W. LaBelle, A study of whistlers correlated with bursts of electron precipitation near $L = 2$, *J. Geophys. Res., 87*, 4427, 1982.

Carpenter, D. L., U. S. Inan, M. L. Trimpi, R. A. Helliwell, and J. P. Katsufrakis, Perturbations of subionspheric LF and MF signals due to whistler-induced electron precipitation bursts, *J. Geophys. Res., 89*, 9857, 1984.

Chang, H. C., and U. S. Inan, A theoretical model study of observed correlations between whistler mode waves and energetic electron precipitation events in the magnetosphere, *J. Geophys. Res., 88*, 10,053, 1983.

Chang, H. C., and U. S. Inan, Lightning-induced energetic electron precipitation from the magnetosphere, *J. Geophys. Res., 90*, 1531, 1985.

Crombie, D. D., A. H. Allen, and N. Newman, Phase variations of 16 kc/s transmissions from rugby as received at New Zealand, *Proc. Inst. Elec. Eng., Part B*, 301, 1958.

Goldberg, R. J., J. R. Barcus, L. C. Hale, and S. A. Curtis, Direct observation of magnetospheric electron precipitation stimulated by lightning, *J. Atmos. Terr. Phys., 48*, 293, 1986.

Goldberg, R. J., S. A. Curtis, and J. R. Barcus, Detailed spectral structure of magnetospheric electron bursts precipitated by lightning, *J. Geophys. Res., 92*, 2505, 1987.

Helliwell, R. A., J. P. Katsufrakis, and M. L. Trimpi, Whistler-induced amplitude perturbation in VLF propagation, *J. Geophys. Res., 78*, 4679, 1973.

Imhof, W. L., E. E. Gaines, H. D. Voss, J. B. Reagan, D. W. Datlowe, J. Mobilia, R. A. Helliwell, U. S. Inan, and J. Katsufrakis, Results from the SEEP active space plasma experiment: Effects on the ionosphere, *Radio Sci., 20*, 511, 1985.

Inan, U. S., and D. L. Carpenter, On the correlation of whistlers and associated subionospheric VLF/LF perturbations, *J. Geophys. Res., 91*, 3106, 1986.

Inan, U. S., and D. L. Carpenter, Lightning-induced electron precipitation events observed at $L \simeq 2.4$ as phase and amplitude perturbations on subionospheric VLF signals, *J. Geophys. Res., 92*, 3293, 1987.

Inan, U. S., D. L. Carpenter, R. A. Helliwell, and J. P. Katsufrakis, Subionospheric VLF/LF phase perturbations produced by lightning-whistler induced particle precipitation, *J. Geophys. Res., 90*, 7457, 1985*a*.

Inan, U. S., H. C. Chang, R. A. Helliwell, W. L. Imhof, J. R. Reagan, and M. Walt, Precipitation of radiation belt electrons by man-made waves: A comparison between theory and measurement, *J. Geophys. Res., 90*, 359, 1985*b*.

Inan, U. S., T. G. Wolf, and D. L. Carpenter, Geographic distribution of lightning-induced electron precipitation observed as VLF/LF perturbation event, *J. Geophys. Res.*, in press, 1988.

Kelley, M. C., C. L. Siefring, R. F. Pfaff, P. M. Kintner, M. Larsen, R. Green, R. H. Holzworth, L. C. Hale, J. D. Mitchell, and D. Le Vine, Electrical measurements in the atmosphere and ionosphere over an active thunderstorm, 1, Campaign overview and initial ionospheric results, *J. Geophys. Res., 90*, 9815, 1985.

Leyser, T., U. S. Inan, D. L. Carpenter, and M. L. Trimpi, Diurnal variation of burst precipitation effects on subionospheric VLF/LF signal propagation near $L = 2$, *J. Geophys. Res., 89*, 9139, 1984.

Lohrey, B., and A. B. Kaiser, Whistler-induced anomalies in VLF propagation, *J. Geophys. Res., 84*, 5121, 1979.

Neubert, T., T. F. Bell, and L. R. O. Storey, Resonance between coherent whistler mode waves and electrons in the topside ionosphere, J. Geophys. Res., 92, 255, 1987.

Orville, R. E., R. A. Weisman, R. B. Pyle, R. W. Henderson, and R. E. Orville, Jr., Cloud-to-ground lightning flash characteristics from June 1984 through May 1985, *J. Geophys. Res., 92*, 5640, 1987.

Park, C. G., and R. A. Helliwell, The formation by electric field of field-aligned irregularities in the magnetosphere, *Radio Sci., 6*, 299, 1971.

Prentice S. A., and D. Mackeras, The ratio of cloud to cloud-ground lightning flashes in thunderstorms, *J. Appl. Meteorol., 16*, 545, 1977.

Tolstoy, A., T. J. Rosenberg, U. S. Inan, D. L. Carpenter, Model predictions of subionospheric VLF signal perturbations resulting from localized electron precipitation induced ionization enhancement regions, *J. Geophys. Res., 92*, 127, 1986.

Voss, H. D., W. L. Imhof, J. Mobilia, E. E. Gaines, M. Walt, U. S. Inan, R. A. Helliwell, D. L. Carpenter, J. P. Katsufrakis, and H. C. Chang, Lightning induced electron precipitation, *Nature, 312*, 740, 1984.

Wait, J. R., Influence of a circular ionospheric depression on VLF propagation, *J. Res. Natl. Bur. Stand., Sect. D, 68*, (8), 907, 1964.

U. S. Inan, D. C. Shafer, and W. Y. Yip, Space, Telecommunications and Radioscience Laboratory, Department of Electrical Engineering, Durand 324, Stanford, CA 94305.

R. E. Orville, Department of Atmospheric Science, State University of New York, Albany, NY 12222.

(Received October 19, 1987;
revised February 29, 1988;
accepted March 9, 1988.)